

CONFIDENTIAL

Copy
RM L56G20a

C1

NACA

RESEARCH MEMORANDUM

CLASSIFICATION CHANGES

UNCLASSIFIED

NASA Class. Change Notices,

AN INVESTIGATION OF A SOURCE OF SHORT-ROUND

Issue no. 4, Aug. 1, 1963.

BEHAVIOR OF MORTAR SHELLS

*Declassified**June 12, 1963.* By John D. Bird and Jacob H. Lichtenstein ✓*APR -10-11-63.*Langley Aeronautical Laboratory
Langley Field, Va.

LIBRARY COPY

OCT 21 1956

LANGLEY AERONAUTICAL LABORATORY
LIBRARY NACA
LANGLEY FIELD, VIRGINIA

CLASSIFIED DOCUMENT

This material contains information affecting the National Defense of the United States within the meaning of the espionage laws, Title 18, U.S.C., Secs. 793 and 794, the transmission or revelation of which in any manner to an unauthorized person is prohibited by law.

NATIONAL ADVISORY COMMITTEE
FOR AERONAUTICS

WASHINGTON

October 26, 1956

CONFIDENTIAL



NATIONAL ADVISORY COMMITTEE FOR AERONAUTICS

RESEARCH MEMORANDUM

AN INVESTIGATION OF A SOURCE OF SHORT-ROUND

BEHAVIOR OF MORTAR SHELLS

By John D. Bird and Jacob H. Lichtenstein

SUMMARY

A low-speed investigation was made in the Langley stability tunnel of the motions of a model of a mortar shell which was mounted with freedom to spin, yaw, and precess. The tests demonstrated that self-sustaining, large-amplitude, whirling motions of the model (short-round behavior) could be obtained for certain model configurations if sufficiently large initial yaw and some spin were present when the model was released. This behavior was attributed to an instability of spin caused by lift hysteresis on the tail fins.

INTRODUCTION

Experience in the use of mortar shells has indicated that occasionally they develop a whirling motion of large amplitude which considerably shortens the range because of the large drag at the high angles of yaw involved. This performance has been termed the short-round phenomenon, and it is a matter of some concern because it may cause shells to fall on friendly troops. References 1 to 3 indicate that an instability of spin (negative roll damping about the body axes) can result in short-round performance if there is a sufficiently large disturbance in yaw.

A few experiments made in the Langley stability tunnel have indicated that an instability of spin of a mortar shell can exist because of an aerodynamic hysteresis effect which makes the tail fins have unstable roll damping at large angles of yaw. In the experiments mentioned, a 6-fin mortar-shell tail assembly was mounted on a shaft and free to spin. This assembly was extended from the tunnel wall in a downstream direction at various angles, and the tendency of the tail assembly to spin was observed. These experiments were prompted by the knowledge that roll instability of lifting surfaces may exist at sufficiently high angles of attack.

████████████████████

The purpose of this investigation was to determine whether this mechanism of spin instability could actually produce short-round performance on a model and to determine the influence of certain geometrical modifications on this phenomenon. The technique employed was that described in reference 4 in which the model was mounted on a gimbal so that it was free to spin, yaw, and precess but was restrained in translation. A model of a mortar shell that had occasionally shown short-round behavior was used for the investigation. This model was tested with various nose and tail configurations to determine the influence of nose shape and fin geometry on the stability of the model.

NOMENCLATURE

The results are presented relative to the Eulerian system of axes shown in figure 1 in which positive directions of spin and angular displacement are indicated by arrows. Certain terms employed frequently in the text are defined as follows:

Spin	rotational motion of shell about longitudinal axis
Angle of yaw	angle between shell longitudinal axis and wind direction
Angle of precession	angular position of plane defined by shell longitudinal axis and wind direction measured in plane perpendicular to wind direction from an arbitrary reference position
X,Y,Z	coordinate axes

APPARATUS AND TESTS

Employed in these tests were a 2.3-scale model of a typical mortar shell (fig. 2), a suitable mounting system, a tripper mechanism which held the model at an angle of yaw until release, and cameras for recording the model motions. Figure 3 shows the model mounted in the test section of the Langley stability tunnel.

The model employed for these tests was constructed, basically, of aluminum bulkheads with a spun magnesium skin 1/16 inch thick. Lead was used for ballast to obtain the proper ratio of roll inertia to yaw inertia, and movable weights were used to maintain the same center-of-gravity location when changes were made to the model configuration. Overall dimensional and inertial characteristics are given in table I.

The inertia values of the model were only approximately $1/5$ the scale values of a typical mortar shell; however, the proper ratio of roll inertia to yaw inertia was maintained. On the assumption of linear theory this difference in inertia results in helix angles of model motion that are about $2\frac{1}{4}$ times the scale values. A few tests were made with 120 pounds of lead added to the model to give the actual scale inertias. These tests were made on a more substantial support strut than was finally employed for the other tests, and strut interference was found to make the results inconclusive in some respects. For this reason these results are not presented.

The front and rear sections of the model were mounted on a shaft that was supported by ball bearings located in the center section (figs. 4 and 5). In order to allow attachment to the supporting system the center section of the model, the exposed portion of which was 13 inches in length, did not spin. This arrangement should make the unstable Magnus effects smaller and cause the model to be more stable than when the entire missile was spinning. This supposition is supported by the fact that force tests on a missile similar to this one indicated that the Magnus moments were appreciably diminished by holding the center portion of the model stationary. Adjacent bulkheads on the stationary and spinning portions of the model were overlapped in order to reduce the leakage between them.

A number of different ancillary components were employed in the tests. These included three nose configurations and six tail-fin configurations. Photographs showing these components are shown as figures 6, 7, and 8. The differences in the various nose configurations are apparent from the photographs. Two of the 12-fin tail configurations were geometrically similar but had fin cants of 0° (tail 1) and 5° (tail 2). One six-fin tail (tail 3) had fins similar to the 12-fin tails; the two other 6-fin tails differed in that the area was doubled in one case by increasing the fin chord (tail 4) and in the other case by increasing the fin span (tail 5). Tail 6 was similar to tail 1 but had a shroud. In addition to tail 1, tails 3, 4, 5, and 6 had a zero cant to the fins.

The model was mounted on a wire support system through a ball-bearing gimbal located at a position corresponding to the normal center-of-gravity location of the shell. This system permitted the model to change angle of yaw and to precess in much the same manner as in free flight (figs. 3 and 4). The friction in the ball-bearing gimbal was kept as low as possible during the tests by the use of a light grade of machine oil. A safety frame made of music wire $1/8$ inch in diameter was placed in the tunnel near the tail of the model to limit the yawing motion to approximately 55° (fig. 3). This constraint was employed to prevent damage to the model and to the gimbal when unstable conditions were encountered.

The release was a device which served to hold the model at a pre-scribed angle of yaw prior to release (fig. 3). The release was connected through a self-aligning ball bearing to a 5/16-inch-diameter trunnion which was attached to the rear of the model in line with its longitudinal axis. This connection permitted the model to spin in response to the action of the airstream prior to release. The release could be located at various positions across the test section in order to simulate various degrees of initial yaw.

A still camera rigged for time exposures and a motion-picture camera were mounted about 60 feet downstream of the model location for making records of the tests. The still camera was used to record the motion of the tail of the model. This was accomplished by the use of a grain-of-wheat bulb attached at the rear of the model in the trunnion employed for holding the model prior to release. With all other lights extinguished, traces of motion of the bulb were obtained during time exposures. These traces are polar plots wherein the radius is proportional to the angle of yaw of the model and the azimuth angle is the amount that the model has precessed (fig. 9). The motion-picture camera was used to check the results of the still camera and to obtain illustrative scenes of the model motion with full illumination.

All tests were conducted in the 6- by 6-foot test section of the Langley stability tunnel at a dynamic pressure of 24.9 pounds per square foot, which corresponds to a Mach number of 0.13 and a Reynolds number of 4×10^6 based upon the model length. Tests were made to determine the effect of changes in the nose configuration, tail configuration, and rates of spin on the dynamic characteristics of the model at initial angles of yaw from 0° to 50° (table II).

When most of the tests were conducted, the model was held at the initial angle of yaw with the wind on for a sufficient period of time for the model to reach spin equilibrium before release. This initial spin was measured by a Strobotac or stopwatch, depending on the rate of spin. Immediately prior to the release of the model the still or motion-picture camera was tripped, and the ensuing motion of the model was recorded. In some cases initial spin by hand (about 100 revolutions per minute) was introduced prior to starting the test to see if spin instability would develop from a small disturbance.

RESULTS AND DISCUSSION

Presentation of Results

A list of all tests conducted, including an index to the figures giving experimental results and certain comments thereon, is given in

table II. All the experimental data were from photographic traces of the bulb attached to the rear of the model. No data are shown where the model touched the safety frame.

Stability of Original Model

The original model (nose 1, tail 1) indicated no spin instability or unstable whirling motion (short-round behavior) for all conditions investigated (table II and fig. 10). The conditions investigated included initial yaw angles to 50° , both with and without the application of initial spin by hand in either direction. The initial spin by hand was about 100 revolutions per minute and was given to determine whether a spin would develop from a small disturbance.

Effect of Canted Fins

Canting the fins of the original model 5° produced a spin rate of about 450 revolutions per minute. Figure 11 shows that this amount of spin was adequate to produce a large-amplitude whirling motion when the model was released at 50° yaw. The frequency of precession or whirling was 0.70 cycle per second. Other runs (table II) indicate that for sufficiently small initial yaw (less than 20°) this configuration was stable (no whirling motion). These results indicate, as would be expected from references 4 to 6, that both spin and an appreciable initial yaw are required for large-amplitude whirling motions to develop.

Effect of Reducing Number of Tail Fins

The model equipped with tail 3 had spin instability when held in the airstream at fixed angles of yaw of 30° , 40° , and 50° (table II). This instability is attributed to an aerodynamic hysteresis associated with the rotation of the tail surfaces, and it is thought to be similar to the loss in roll damping of wings which occurs at high angles of attack. In the cases of 30° and 40° yaw, the model rotated at -112 and -300 revolutions per minute, respectively, prior to release. When the model was permitted to spin up prior to release, a large-amplitude whirling motion developed for initial yaw angles of 40° and 50° (fig. 12). The frequency of this whirling or precessional motion was 0.85 cycle per second. The initial yaw angle of 30° was critical in this respect in that the motion after release was stable in some cases (fig. 12(a)) and unstable (or whirling) in others (table II, test 9). When the model was released prior to spin up at 50° yaw, the motion was found to precess for a long time but to damp slowly to about zero yaw; this result indicated that this case was marginally stable (fig. 13).

An examination of these results indicates that the large-amplitude motion encountered is basically that obtained in reference 4, wherein the whirling motion is maintained by the presence of the Magnus moment associated with spin and wake asymmetry. In the case of the uncanted fins used on this model the spinning motion is maintained by the basic instability of the fins rather than by the cant.

The resonance phenomenon discussed in reference 7 should not contribute to the behavior of this model since the ratio of yaw to spin frequency was very small for all configurations investigated (table I and table II); thus, the region of resonance instability was not approached. It is interesting to note that the oscillatory damping of the nonspinning model is the same with the 6- and 12-fin tails (table I).

Effect of Sharp Noses

Adding a sharp nose (nose 2) to the model fitted with tail 3 appears to decrease the directional stability and damping for the low range of yaw angles in that a circular wandering motion at about 25° yaw was obtained when the model was released at 0° yaw (fig. 14). In some cases the model trimmed at about 20° yaw for long periods. If the model were held at 40° yaw until the spin was well developed, a whirling motion at 0.81 cycle per second was obtained that was about 40° in amplitude, as was the case for the model with the basic nose (nose 1) and tail 3.

Experiments with a longer, pointed nose (nose 3) gave results (fig. 15 and table II) similar to those obtained for the shorter, pointed nose. An interesting result was obtained when the model was released from 50° yaw before spin had developed (fig. 16). In this case, possibly because of low directional stability and the effect of vorticity shed from the pointed nose, an extremely erratic large-amplitude motion was obtained.

Effect of Tail Area and Shrouding For

Pointed-Nose Model (Nose 3)

Model configurations with tails composed of six fins having twice the area of tail 3 but with aspect ratios of one-half the value for tail 3 (tail 4) and twice the value for tail 3 (tail 5) did not show the spin instability and large-amplitude whirling motion which was obtained for the model with tail 3. (See table II and fig. 17.) The low-aspect-ratio tail (tail 4) showed a greater tendency to spin when the model was held at large yaw angles than the high-aspect-ratio tail (tail 5), however. An experiment with a shrouded tail (tail 6) did not show spin instability or large-amplitude whirling when the model was held at 50° yaw and released (table II, fig. 17). From these results it appears that either increasing

the tail area or adding a shroud to the tail would be beneficial with regard to dynamic behavior.

CONCLUSIONS

From an investigation conducted in the Langley stability tunnel of the motions of a model of a mortar shell which was mounted with freedom to spin, yaw, and precess, the following observations were made:

1. The tests demonstrated that large-amplitude whirling motions of the model (short-round behavior) could be obtained for certain model configurations if sufficiently large initial yaw and some spin were present when the model was released. This whirling motion would not persist without the existence of an instability of spin or a cant of the tail fins for the cases investigated.

2. Spin instability was obtained for only 6-fin tail surfaces composed of fins having an aspect ratio of about 1. Tail surfaces having 12 fins of aspect ratio 1, as are sometimes employed for mortar shells, did not exhibit spin instability under the conditions of these tests. Increasing the tail area tended to reduce the instability of spin. The instability of spin obtained in this investigation was felt to result from an aerodynamic hysteresis associated with the rotation of the tail surfaces.

Langley Aeronautical Laboratory,
National Advisory Committee for Aeronautics,
Langley Field, Va., July 5, 1956.

REFERENCES

1. Zaroodny, Serge J.: On the Mechanism of Dispersion and Short Ranges of Mortar Fire. With an Appendix on an Alternate Solution of the Equations of Motion of a Yawing Projectile. Rep. No. 668, Ballistic Res. Labs., Aberdeen Proving Ground, Apr. 7, 1948. *u*
2. Zaroodny, S. J.: On the Dispersion and Short Ranges of Mortar Fire. Memo Rep. No. 685, Ballistic Res. Labs., Aberdeen Proving Ground, July 1953. *u* *N-25768*
3. Zaroodny, Serge J.: Failure of the Instability of Spin of the First Kind. Memo Rep. No. 832, Ballistic Res. Labs., Aberdeen Proving Ground, Sept. 1954. *u* *N-33987*
4. Bird, John D., and Lichtenstein, Jacob H.: Wind-Tunnel Experiments Concerning the Dynamic Behavior of a Low-Speed Slowly Spinning Fin-Stabilized Rocket. NACA RM L54D22, 1954. *C*
5. Cohen, C. J., and Hubbard, E. C.: Predictions of the Motion of a Slowly Spinning Research Rocket. NPG Rep. 1421, U. S. Naval Proving Ground (Dahlgren, Va.), Nov. 30, 1955. *u* *N-21076*
6. Schmidt, J. M.: Analog Computer Simulation of Flight Characteristics of Two 90 MM Fin Stabilized Shell T108E40 and T316. Memo Rep. No. 953, Ballistic Research Labs., Aberdeen Proving Ground, Dec. 1955. *u* *CD-41609*
7. Phillips, William H.: Effect of Steady Rolling on Longitudinal and Directional Stability. NACA TN 1627, 1948. *u*

TABLE I
DIMENSIONAL AND INERTIAL CHARACTERISTICS

Characteristics	Mortar shell	Model
Weight, lb	11.2	-----
Moment of inertia about longitudinal axis, slug-ft ² . .	0.003	0.037
Moment of inertia about lateral axis, slug-ft ²	0.062	0.782
Length of basic model, ft	1.9	4.4
Maximum diameter, ft	0.26	0.60
Distance from flat of normal nose (nose 1) to center of gravity, ft	0.83	1.91
Forward velocity at peak of trajectory, fps	270	145
Natural frequency in yaw of nonspinning model equipped with nose 1 and either tail 1 or 3, cps . . .	-----	0.41
Time for an initial disturbance of nonspinning model equipped with nose 1 and either tail 1 or 3 to damp to half-amplitude, sec	-----	1.43

TABLE II
TEST CONDITIONS AND RESULTS

Test number	Data on figure	Nose configuration	Tail configuration	Initial yaw, deg	Initial spin by hand	Rotational speed at release, rpm (1)	Spin behavior	Motion behavior
1	10(a)	1	1	40	None	0	Stable	Stable, trimmed at zero yaw on release
2	10(b)	1	1	50	None	0	Stable	Stable, trimmed at zero yaw on release
3	10(c)	1	1	40	Right	105	Stable	Stable, trimmed at zero yaw on release
4	10(d)	1	1	50	Right	Decreasing	Stable	Stable, trimmed at zero yaw on release
5	10(e)	1	1	40	Left	135	Stable	Stable, trimmed at zero yaw on release
6	10(f)	1	1	50	Left	Decreasing	Stable	Stable, trimmed at zero yaw on release
7	11	1	2, Canted fins	50	None	450	Stable	Precessed at about 30° yaw
8	-----	1	2, Canted fins	0 to 20	None	450	Stable	Stable below 20° yaw at release
9	12(a)	1	3	30	None	-112	Unstable	Started spinning quickly - generally stable but would precess at large amplitude occasionally
10	12(b)	1	3	40	None	-300	Unstable	Precesses at about 40° yaw, slow to start spinning
11	12(c)	1	3	50	None	Not measured	Unstable	Precesses at about 40° yaw, slow to start spinning
12	13	1	3	50	None	Not measured	Unstable	Stable, released before spin develops
13	14(a)	2	3	0	None	0	Stable	Fairly large-amplitude, slow, irregular motion
14	14(b)	2	3	40	None	325	Unstable	Precessed at about 40° yaw
15	15(a)	3	3	30	None	60	Unstable	Stable, trimmed at about 15° yaw on release
16	15(b)	3	3	40	None	-350	Unstable	Precessed at about 40° yaw
17	15(c)	3	3	50	None	500	Unstable	Precessed at about 40° yaw
18	16	3	3	50	None	0	Unstable	Stable, released before spin developed, performed erratic motion and trimmed at about 15° yaw
19	17(a)	3	4	50	Right	Decreasing	Stable	Stable, trimmed at zero yaw on release
20	17(b)	3	5	50	None	0	Stable	Stable, would not spin, trimmed at zero yaw on release
21	17(c)	3	6	50	Right and left	0	Stable	Stable, would not sustain a spin, trimmed at zero yaw on release

¹Signs indicate direction of rotation where (+) is clockwise or right rotation (viewed from rear of model) and (-) is counterclockwise or left rotation.

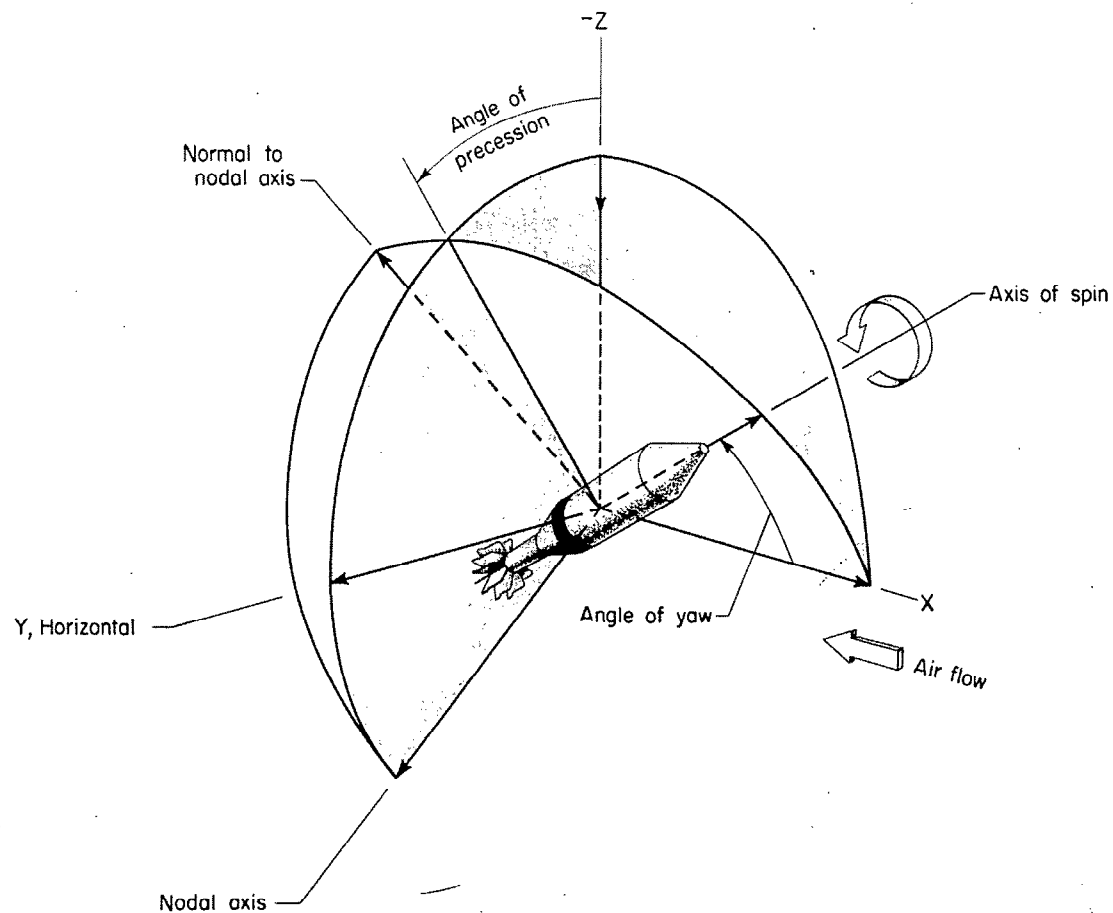


Figure 1.- System of axes used to define spin, yaw, and precession.

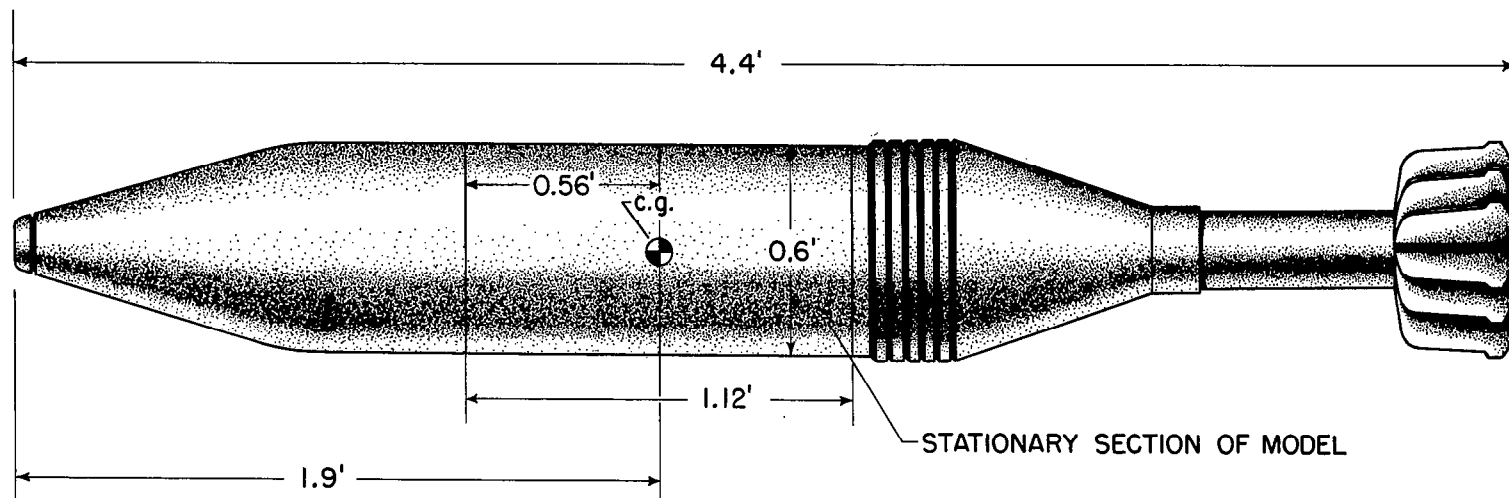
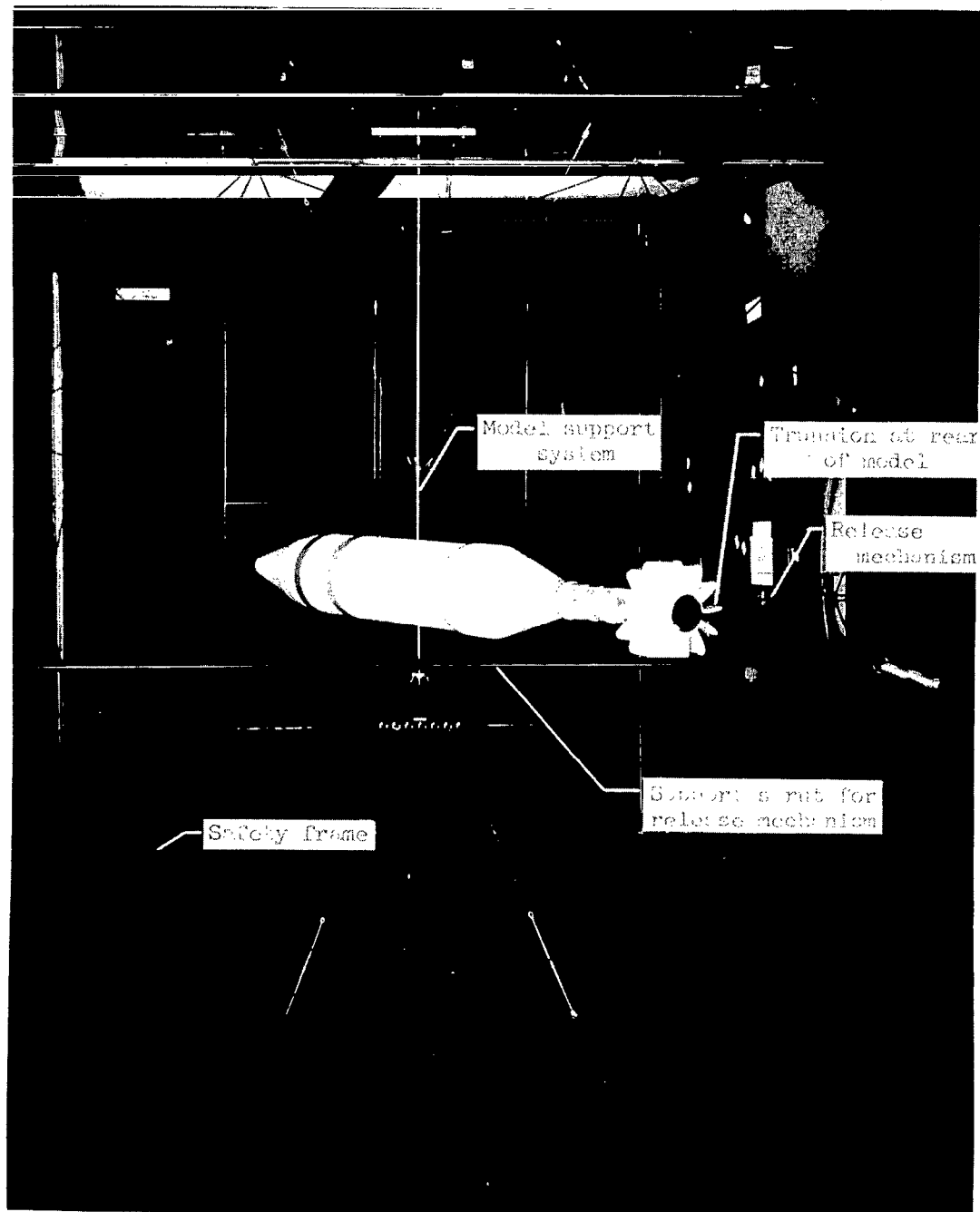
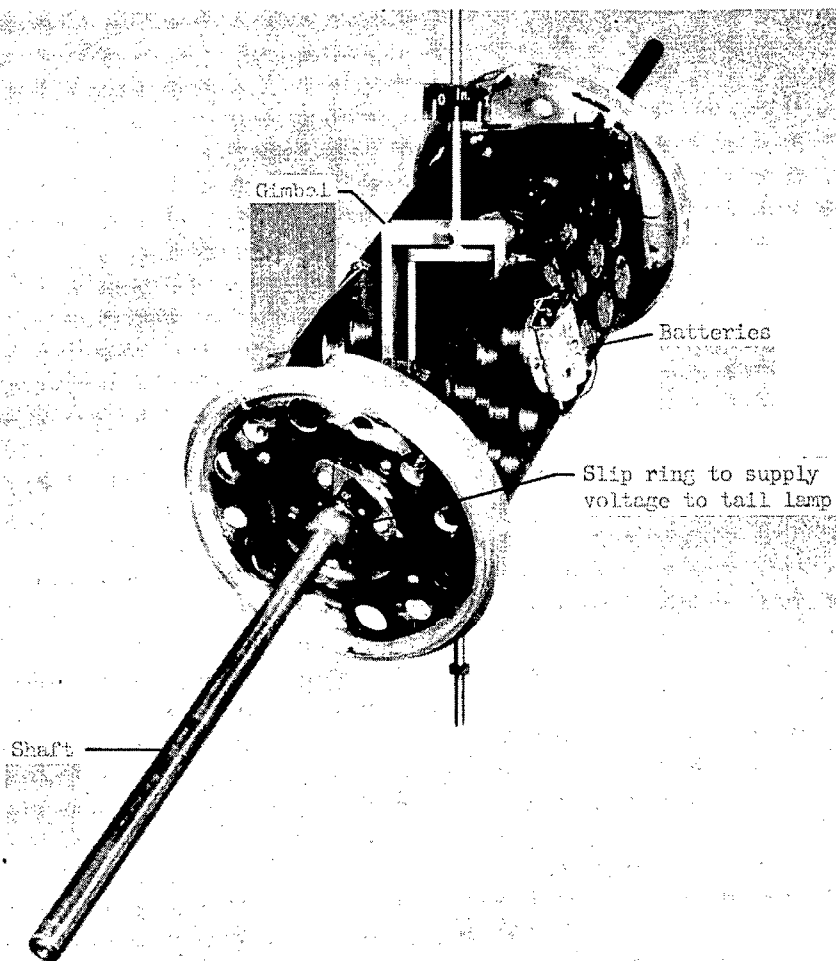


Figure 2.- Dimensions of model.

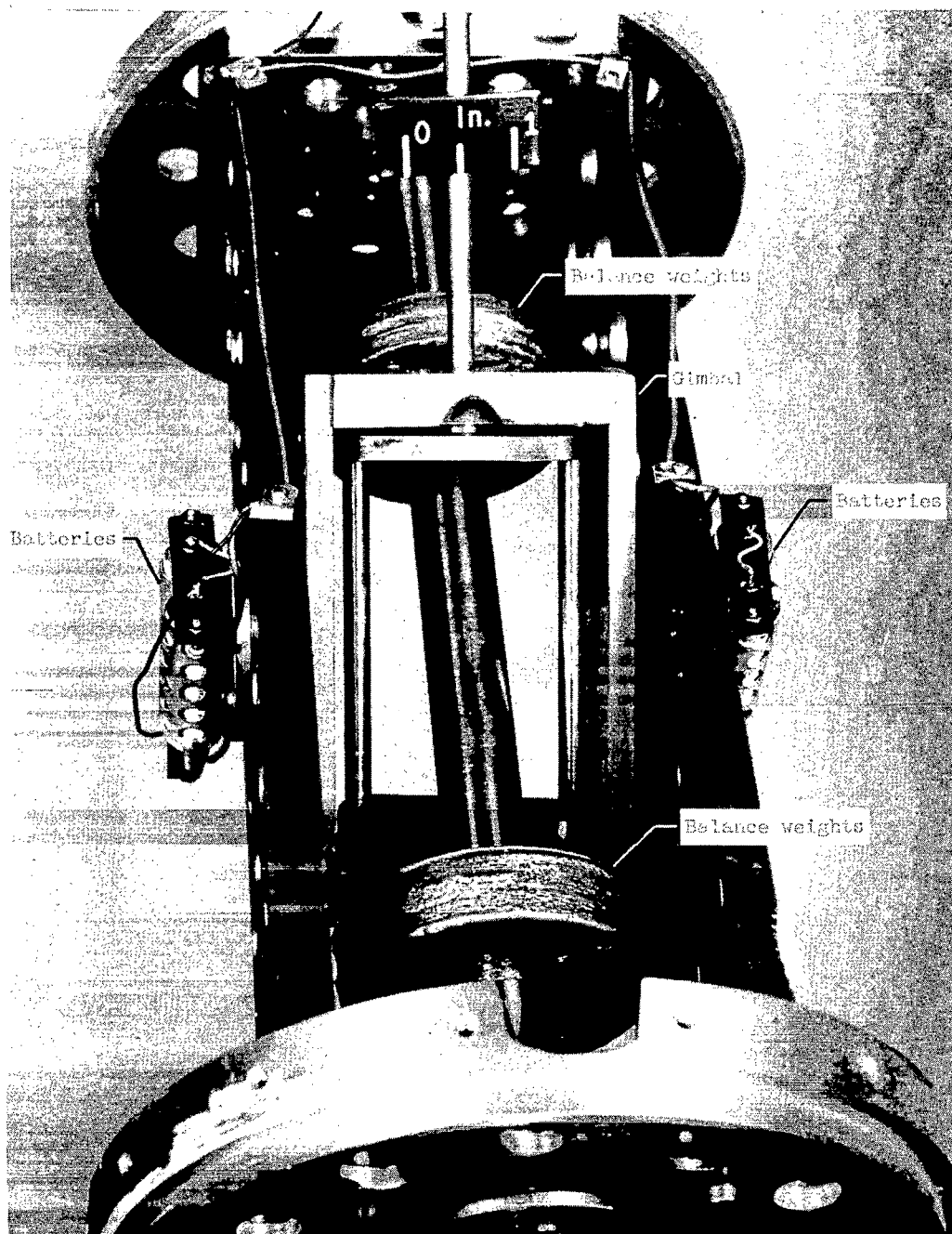


L-91906.1
Figure 3.- Photograph of the test setup in the Langley stability tunnel showing the model and release arrangement.



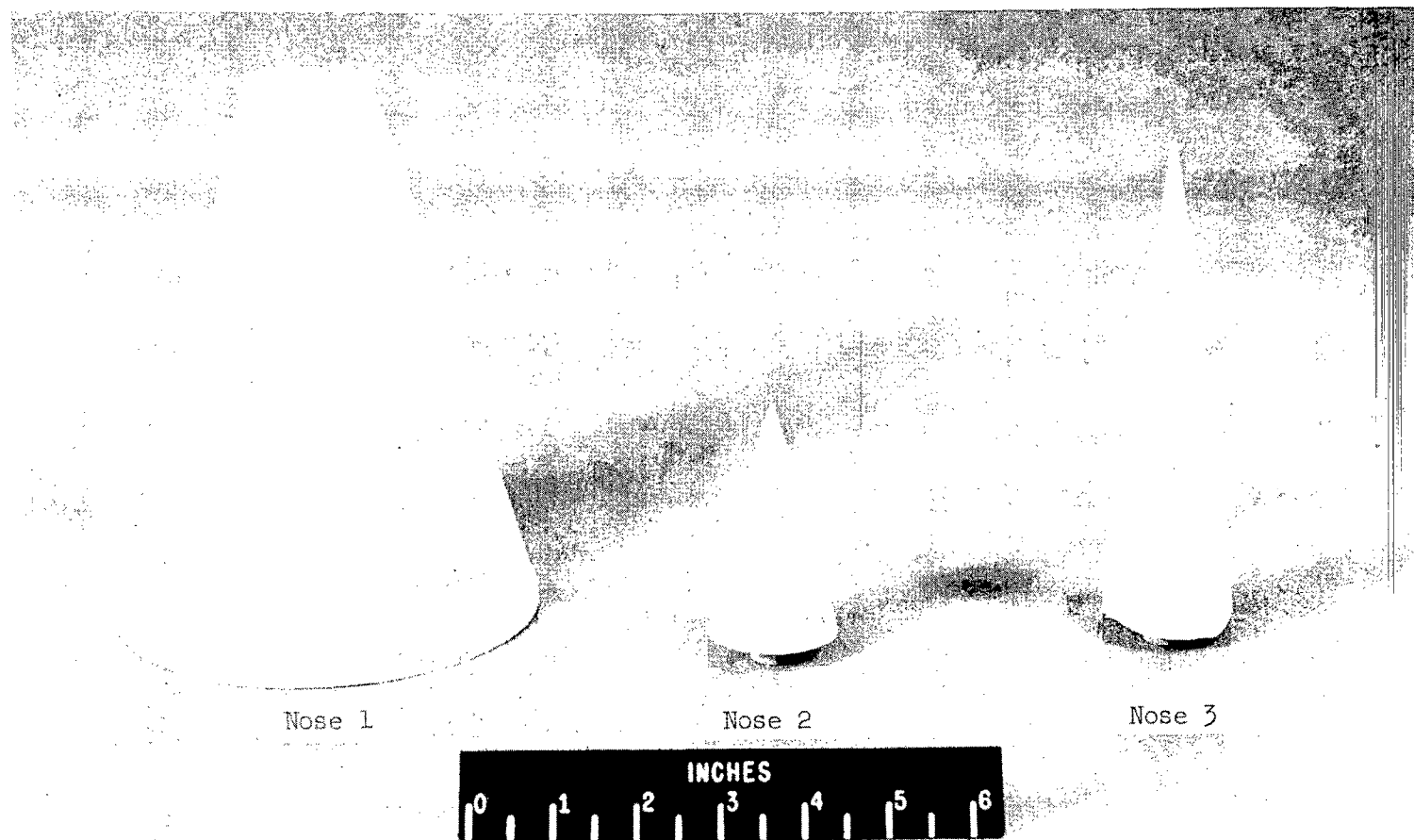
L-92660.1

Figure 4.- Photograph of the internal structure of the model showing the shaft on which the rotating front and rear portions of the model were mounted.



L-92661.1

Figure 5.- Photograph of the internal structure of the model showing the gimbal system, the balance weights, and the batteries for the tail light.

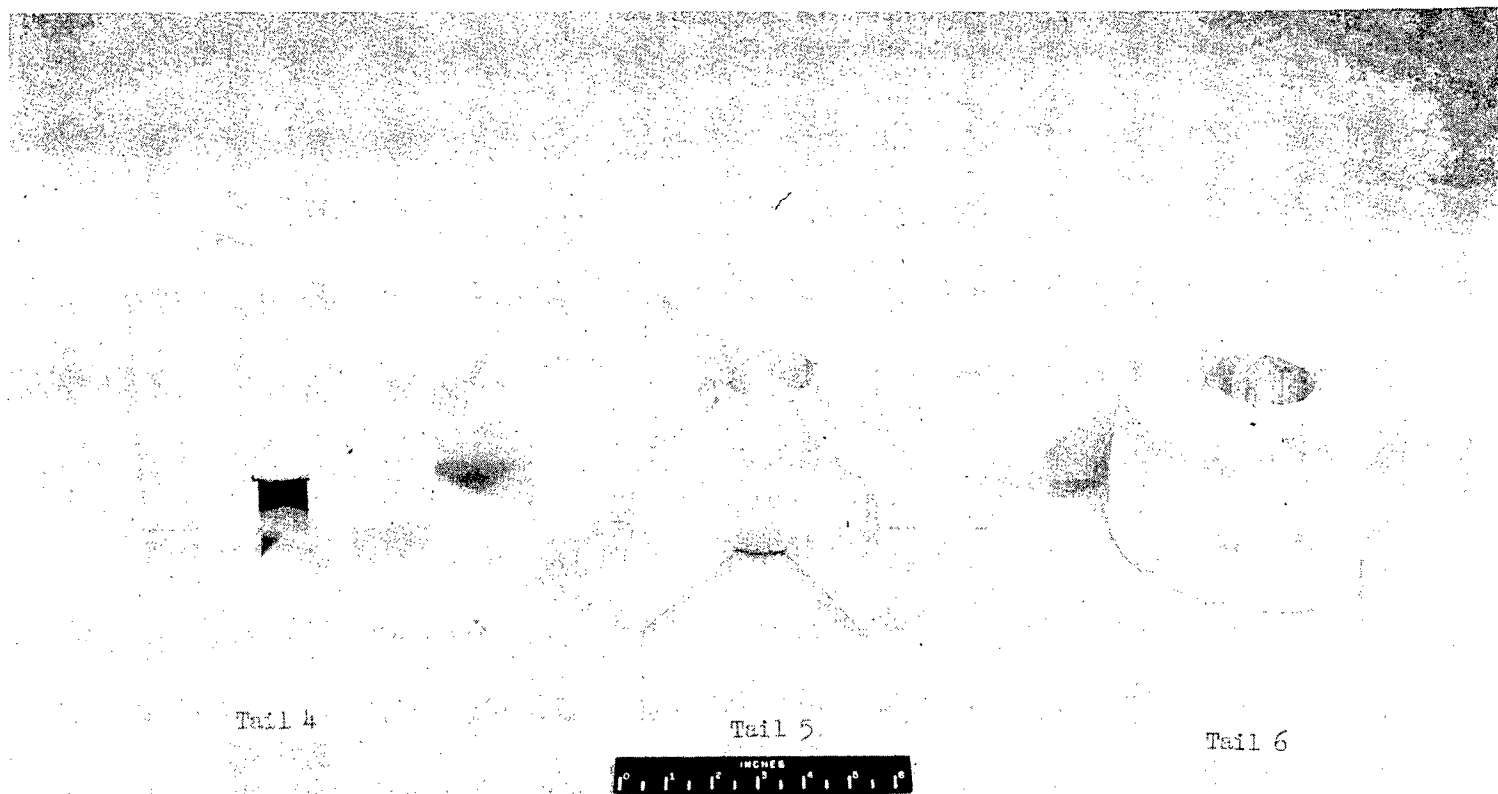


L-92853.1
Figure 6.- Model noses used in tests. Noses 2 and 3 were added to end
of nose 1 when used.



L-93093.1

Figure 7.- Model tails used in most of the tests. Tails 1 and 3 have 0° cant of the fins. Tail 2 has fins canted 5° to axis of mortar shell to produce counterclockwise spin when viewed from downstream.



L-93092.1
Figure 8.- Model tails used in tests to determine effect of tail modifications. Tails 4, 5, and 6 have 0° cant of the fins.

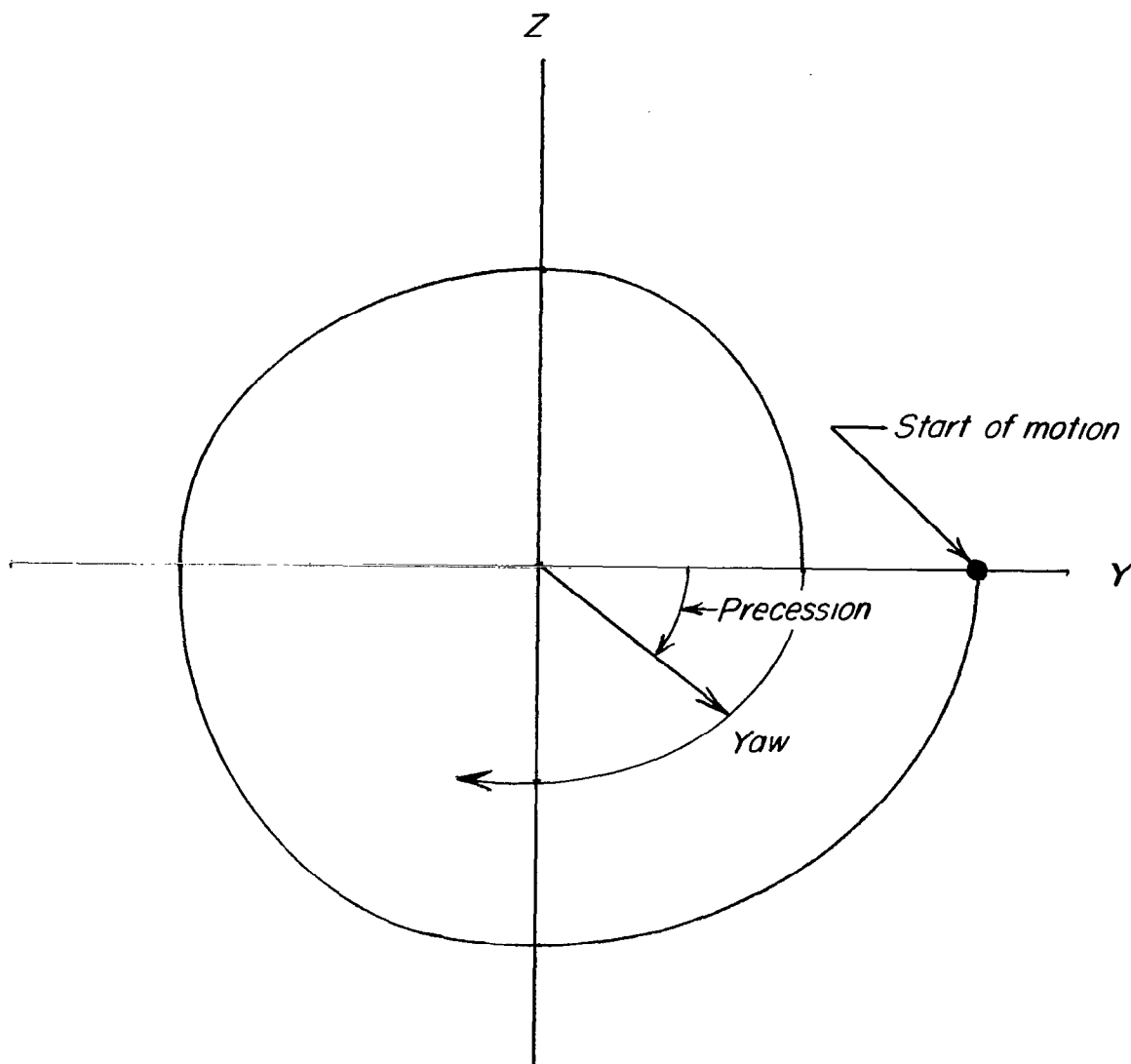
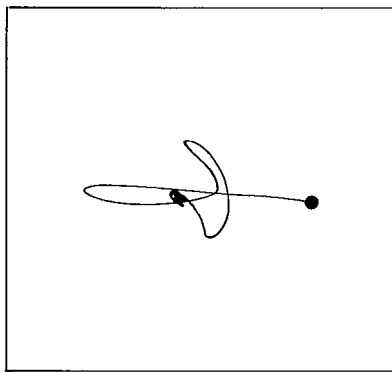
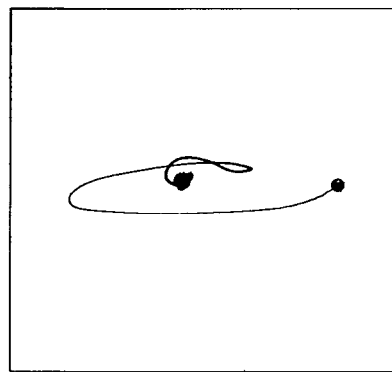


Figure 9.- Typical trace of model motion showing the angles of yaw and precession.

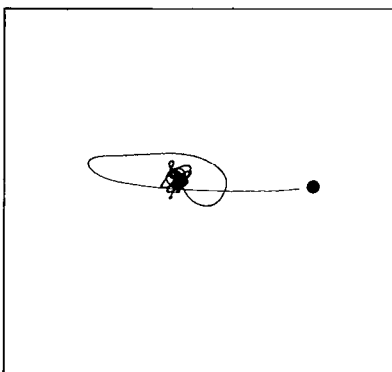
~~CONFIDENTIAL~~



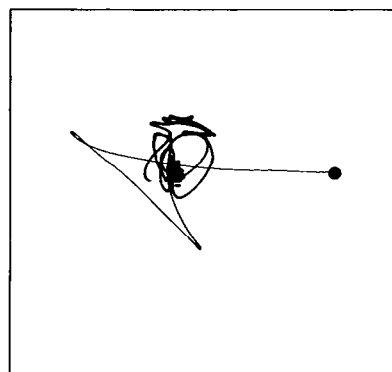
(a) Initial yaw angle 40° ;
no initial spin.



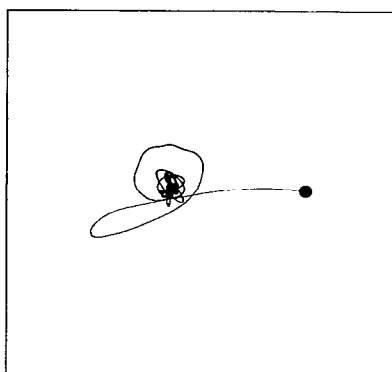
(b) Initial yaw angle 50° ;
no initial spin.



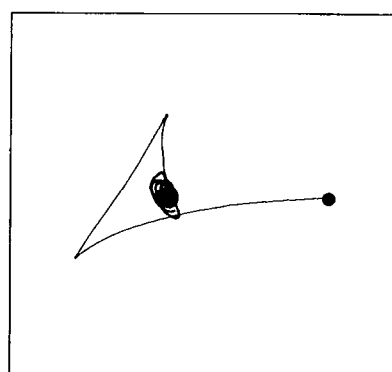
(c) Initial yaw angle 40° ;
initial spin clockwise.



(d) Initial yaw angle 50° ;
initial spin clockwise.



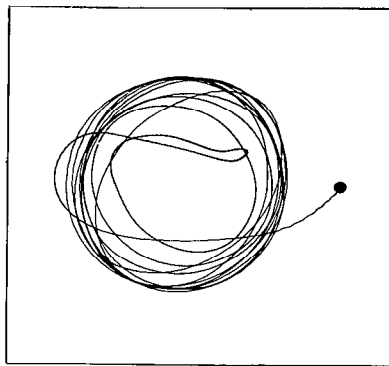
(e) Initial yaw angle 40° ; ini-
tial spin counterclockwise.



(f) Initial yaw angle 50° ; ini-
tial spin counterclockwise.

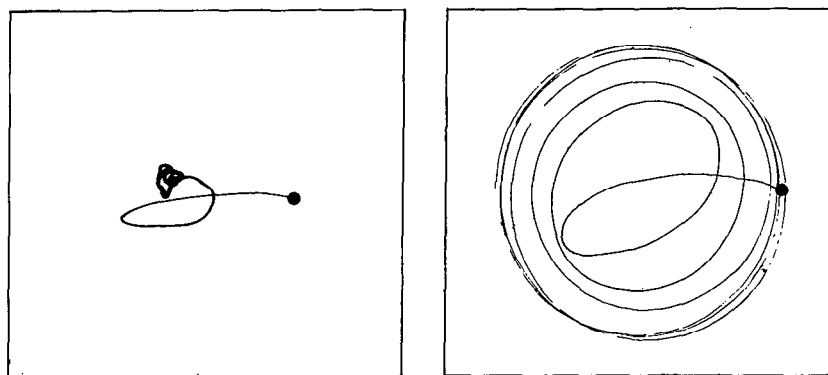
Yaw scale 0° 20° 50°

Figure 10.- Experimental motion of model equipped with nose 1 and tail 1 for two initial angles of yaw. Dots indicate points of release.

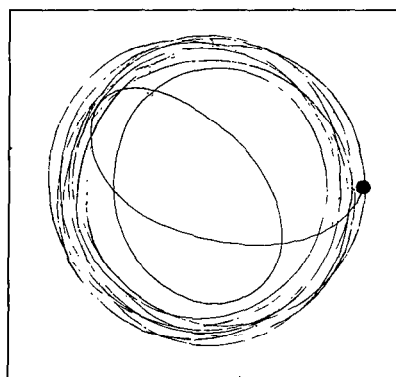


Yaw scale 0° 20° 50°

Figure 11.- Experimental motion of model equipped with nose 1 and tail 2 (canted fins) for an initial yaw angle of 50° . No impressed initial spin. Spin at release about 450 revolutions per minute counterclockwise. Dot indicates point of release.



(a) Initial yaw angle 30° ; spin at release 112 revolutions per minute counterclockwise. (b) Initial yaw angle 40° ; spin at release 300 revolutions per minute counterclockwise.



(c) Initial yaw angle 50° ; spin at release clockwise.

Yaw scale 0° 20° 50°

Figure 12.- Experimental motion of model equipped with nose 1 and tail 3 (6 fins) for initial yaw angles of 30° , 40° , and 50° . No impressed initial spin. Dots indicate points of release.

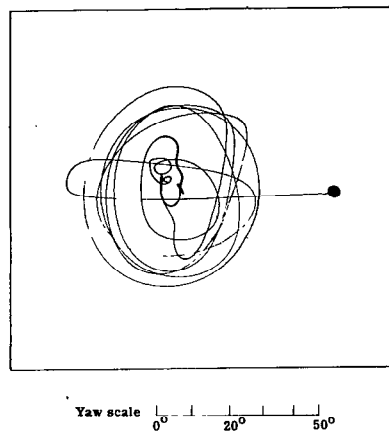
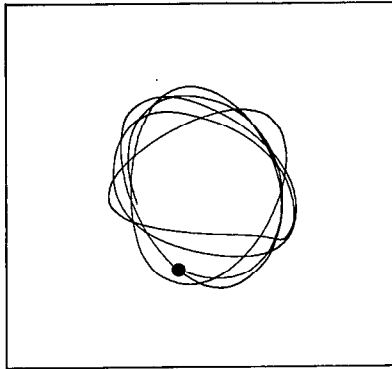
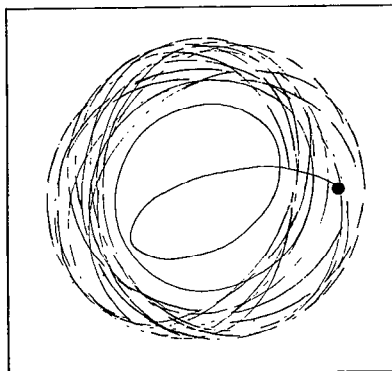


Figure 13.- Experimental motion of model equipped with nose 1 and tail 3 (6 fins) for an initial yaw angle of 50° . Model released before development of spin. Dot indicates point of release.



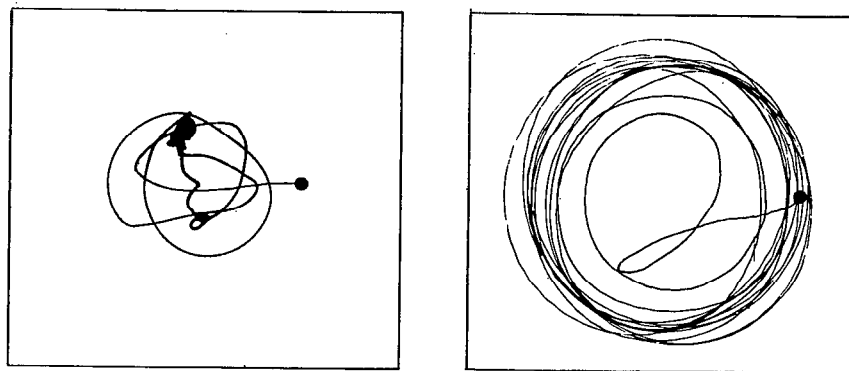
(a) Motion that may ensue when model is released at zero yaw angle with no spin (see table II).



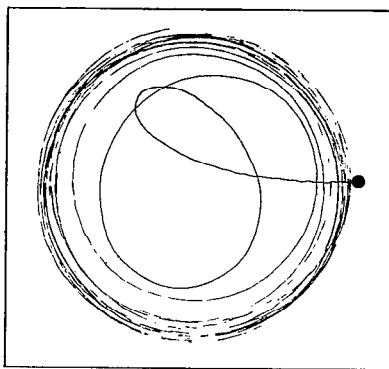
(b) Initial yaw angle 40° ; no impressed initial spin; spin at release 325 revolutions per minute counterclockwise.

Yaw scale 0° 20° 50°

Figure 14.- Experimental motion of model equipped with nose 2 and tail 3 (6 fins) for 2 initial yaw angles. Dot indicates point of release.



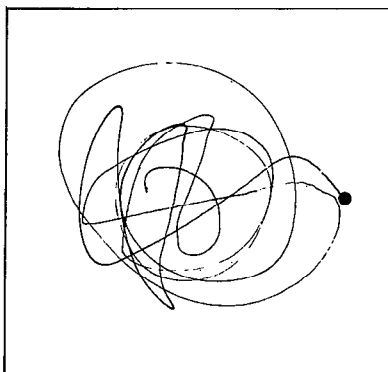
- (a) Initial yaw 30° ; spin at release 60 revolutions per minute clockwise. (b) Initial yaw 40° ; spin at release 350 revolutions per minute counterclockwise.



- (c) Initial yaw 50° ; spin at release 500 revolutions per minute clockwise.

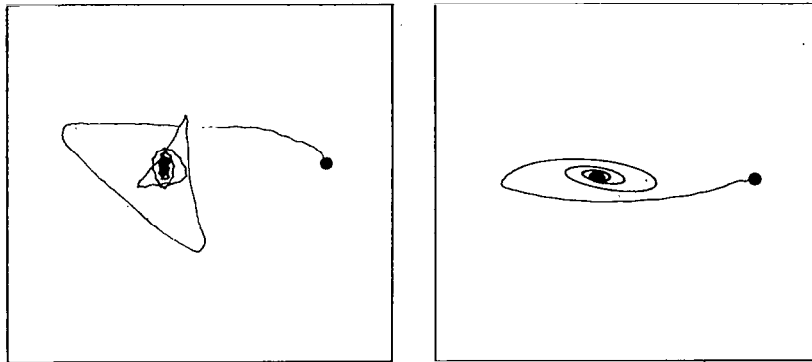
Yaw scale 0° 20° 50°

Figure 15.- Experimental motion of model equipped with nose 3 and tail 3 (6 fins) for several initial yaw angles. No impressed initial spin. Dots indicate points of release.

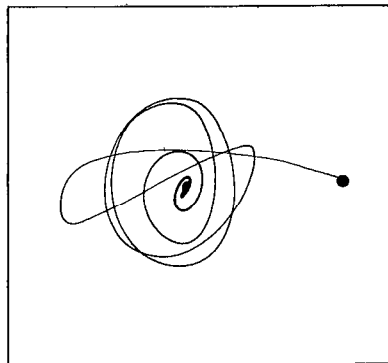


Yaw scale 0° 20° 50°

Figure 16.- Experimental motion of model equipped with nose 3 and tail 3 (6 fins) for an initial yaw angle of 50° . Model released before development of spin. Dot indicates point of release.



(a) Tail 4; impressed initial spin clockwise; spin was dying out on release. (b) Tail 5; no impressed initial spin; no spin on release.



(c) Tail 6; no spin on release.

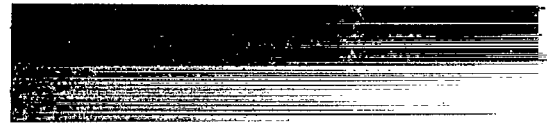
Yaw scale 0° 20° 50°

Figure 17.- Experimental motion of models equipped with nose 3 and various tails for an initial yaw angle of 50° . Dots indicate points of release.

NASA Technical Library



3 1176 01437 2420



CONFIDENTIAL